ACS Medicinal Chemistry Letters

Letter

Cite This: ACS Med. Chem. Lett. 2019, 10, 1393−1399

pubs.acs.org/acsmedchemlett

Peptide-Cleavable Self-immolative Maytansinoid Antibody−Drug Conjugates Designed To Provide Improved Bystander Killing

Juliet A. Costoplus, Karen H. Veale, Qifeng Qiu, Jose F. Ponte, Leanne Lanieri, Yulius Setiady, Ling Dong, Anna Skaletskaya, Laura M. Bartle, Paulin Salomon, Rui Wu, Erin K. Maloney, Yelena V. Kovtun, Olga Ab, Kate Lai, Ravi V. J. Chari, and Wayne C. Widdison*

ImmunoGen, Inc., 830 Winter Street, Waltham, Massachusetts 02451, United States

Supporting Information

ABSTRACT: A new type of antibody−drug conjugate (ADC) has been prepared that contains a sulfur-bearing maytansinoid attached to an antibody via a highly stable tripeptide linker. Once internalized by cells, proteases in catabolic vesicles cleave the peptide of the ADC's linker causing self-immolation that releases a thiol-bearing metabolite, which is then *S*-methylated. Conjugates were prepared with peptide linkers containing only alanyl residues, which were all L isomers or had a single D residue in one of the three positions. A D-alanyl residue in the linker did not significantly impair a conjugate's cytotoxicity or bystander killing unless it was directly attached to the immolative moiety. Increasing the number of methylene units in the maytansinoid side chain of a conjugate did not typically affect an ADC's cytotoxicity to targeted cells but did increase bystander killing activity. ADCs with the highest *in vitro* bystander killing were then evaluated *in vivo* in mice, where they displayed improved efficacy compared to previously described types of maytansinoid conjugates.

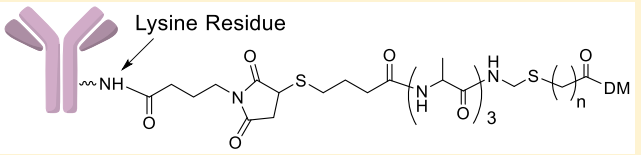

KEYWORDS: *Antibody−drug conjugates, maytansinoid, peptide*

Antibody−drug conjugates (ADCs) are composed of an antibody attached to a cytotoxic payload via a linker.[1,2] Most ADCs bind to target antigens expressed on the surface of cancer cells, then the conjugate internalizes into catabolic vesicles where the antibody, and possibly the linker, are degraded to release one or more cytotoxic metabolites. In some cases, these released metabolite(s) are membrane permeable, allowing them to diffuse into and kill neighboring cells in a tumor, an effect known as bystander killing.[3] ADCs have been investigated for more than two decades; however, ado-trastuzumab emtansine (Kadcyla), for the treatment of metastatic breast cancer, is currently the only conjugate approved for a solid tumor indication.[4] It is a maytansinoid bearing ADC that has a noncleavable linker and releases a charged metabolite that does not induce bystander killing.[1] The high stability of noncleavably linked ADCs is expected to maximize delivery of cytotoxic molecules to tumors while reducing payload release in healthy tissues.[2] However, the linker may not be ideal as many other conjugates using the same linker and payload as ado-trastuzumab emtansine were not successful in the clinic.[5] Also, based on mouse xenograft studies, cleavably linked conjugates that induce bystander killing are typically more efficacious than noncleavably linked ADCs.[6,7]

We have previously developed two types of maytansinoid ADCs that induce bystander killing, each have strengths but also potential for improvement. In the first type, the payload is linked to a lysine residue of an antibody via a disulfide bond, ADCs (**1a−1d**) are shown as examples, Figure 1A.[8] After internalization by cells, the antibody of the ADC is catabolized to give **2** and most is reduced to give the thiol-containing maytansinoid (**3a**), some of which can then be *S*-methylated to **3b**. Only **3a** and **3b** are hydrophobic, allowing them to diffuse into and kill bystander cells. Most of **3a** that reaches the liver *in vivo* is *S*-methylated to **3b**, which is efficiently oxidized to less potent compounds, potentially reducing systemic toxicity.[9] We have previously shown that disulfide-linked ADCs typically show superior efficacy in mouse tumor xenograft models than conjugates bearing the same noncleavable linker used in ado-trastuzumab emtansine.[6] The second type of maytansinoid conjugate that induces bystander killing has a peptide-anilino linkage, such as **4a−4c**, Figure 1B.[10] These ADCs are catabolized by cells to give the potent metabolite **5**, which can induce bystander killing. However, linker half-lives of both disulfide-linked and anilino conjugates were only ∼5.5 days,[10] which compares poorly to the stability of noncleavably linked conjugates (9.3 day).[11]

ADCs can incorporate peptide linkers without anilino moieties; however, in order to maximize metabolite hydrophobicity, the conjugate should release noncharged compounds. Although their work was not on ADCs, Kingsbury and coauthors reported that a peptide could be enzymatically cleaved followed by immolation of the resulting hydrophilic amine to give a hydrophobic thiol-bearing compound.[12] Based on these findings, the goal of this work was to design highly

Received: July 9, 2019
Accepted: September 27, 2019
Published: September 27, 2019

DOI: 10.1021/acsmedchemlett.9b00310
ACS Med. Chem. Lett. 2019, 10, 1393−1399

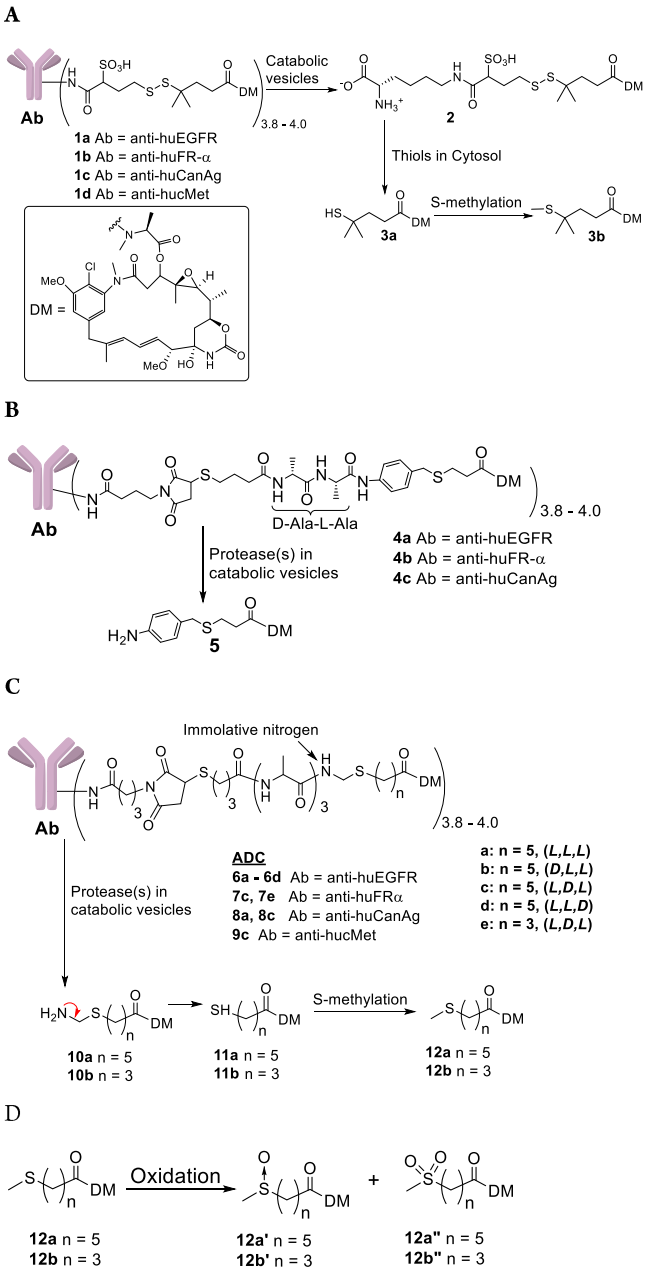

Figure 1. (A) Structures of ADCs bearing disulfide linkers and the metabolites that are formed from their proteolysis in catabolic vesicles followed by disulfide cleavage and *S*-methylation. DM indicates the depicted maytansinoid moiety, derivatizable on the *N*-methyl alanyl amine. (B) Structures of ADCs with peptide-anilino linkers and the metabolite that is formed from proteolysis. (C) Structures of the new ADCs bearing peptide-immolative linkers and the metabolites that are expected to be formed in catabolic vesicles followed by *S*-methylation. Bracketed letters (L or D) indicate alanyl stereochemistry in the direction from antibody toward the maytansinoid. (D) Structures formed if the sulfur atoms of **12a**−**12c** are oxidized.

stable protease cleavable maytansinoid conjugates that release hydrophobic metabolites, capable of bystander killing, and determine if they are superior to disulfide-linked and anilino ADCs.

The humanized mAbs anti-huEGFR (targeting human epidermal growth factor 1),[13] anti-huFRα (targeting human folate receptor-alpha),[14] anti-huCanAg (targeting human CanAg antigen),[15] and anti-hucMet (targeting human cMet antigen)[16] were used in these studies. New immolative ADCs **6a**−**6d** (Ab = anti-huEGFR), **7c**, **7e** (Ab = anti-huFRα), **8a**, **8c** (Ab = anti-huCanAg), and **9c** (Ab = anti-hucMet) with tripeptide linkers were prepared, Figure 1C. After internalization into targeted Ag+ cells, the new ADCs were designed to be cleaved in lysosomes up to the immolative nitrogen atom, followed by release of the corresponding thiol-containing metabolite (**11a** or **11b**), which in turn could potentially be *S*-methylated giving maytansinoids (**12a** or **12b**). In order to simplify the interpretation of results, alanine was the only amino acid residue used in the linkers. Peptide linkers can often be stabilized by replacing an L-amino acid with its D-isomer.[10,17] Thus, the effect of replacing one of the linker L-alanyl residues with its D isomer was investigated. Linker amino acids are listed in the direction from the antibody toward the maytansinoid, for example, (L, L, D) indicates that a D-alanyl residue is directly attached to the immolative nitrogen. Increasing a molecule's hydrophobicity typically improves its diffusion into cells.[18] Therefore, we wished to determine if changing the number of hydrophobic methylene units in the maytansinoid side chain, **n**, would affect ADC bystander killing.

Immolative ADC payloads were prepared as depicted in Scheme 1. Maytansinol (**13**) was reacted with the carbonic

Scheme 1. Synthesis of New Immolative Maytansinoid ADCs[a]

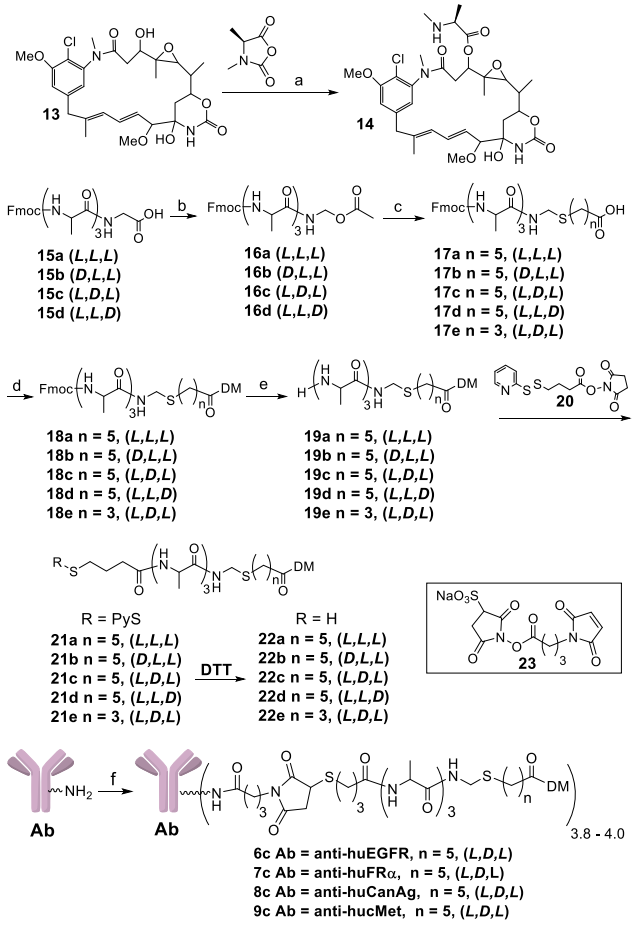

[a]Reagents and conditions: (a) $Zn(OTf)_2$, DIPEA; (b) $Pb(OAc)_4$, AcOH; (c) HS-$(CH_2)_n$-COOH, TFA; (d) EDC, **14**; (e) morpholine; (f) **22c**, **23**.

DOI: 10.1021/acsmedchemlett.9b00310
ACS Med. Chem. Lett. 2019, 10, 1393−1399

anhydride of *N*-methyl alanine in the presence of zinc triflate and *N*,*N*-diisopropylethylamine (DIPEA) to give **14**.[19] Fmoc-protected alanyl peptides (**15a**–**15d**) were prepared by solid phase synthesis,[20] then oxidatively decarboxylated with lead tetraacetate and acetic acid in dimethylformamide (DMF) to give **16a**–**16d** respectively.[21] Compounds **16a**–**16e** were reacted with the appropriate thiol-bearing carboxylic acid in the presence of ∼20% trifluoroacetic acid (TFA) in dichloromethane to give **17a**–**17e**. Compound **14** was coupled to **17a**–**17e** using 1-ethyl-3-(3-(dimethylamino)propyl)-carbodiimide (EDC) to give **18a**–**18e**, which were then deprotected with morpholine giving **19a**–**19e**. The heterobifunctional linker (**20**) was coupled to **19a**–**19e** to give **21a**–**21e**, and disulfide reduction with 1,4-dithiothreitol (DTT) gave payloads (**22a**–**22e**). Immolative ADCs were prepared from one of these payloads and a mAb, as depicted for representative conjugations with **22c**, Scheme 1. The heterobifunctional linker **23** was coupled to the thiol of **22c** in a solution of buffer–organic solvent. The reaction solution, without purification, was reacted with a mAb, and the mixture was purified by size exclusion chromatography (SEC). Disulfide-linked and peptide anilino ADCs as well as their metabolites were prepared as previously described.[10,22]

The compounds that were expected to be formed when cells metabolize immolative ADCs were prepared as depicted in Figure 2. Compound **14** was reacted with 6-mercaptohaxanoic

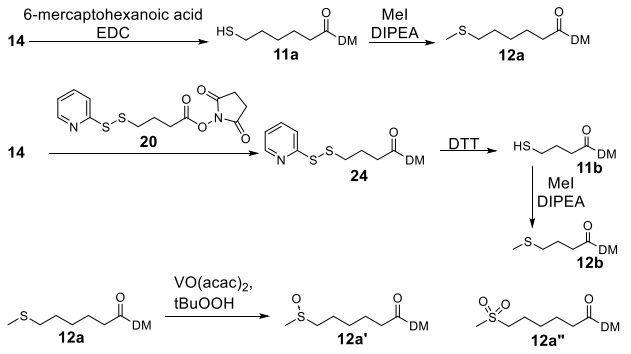

Figure 2. Preparation of possible immolative ADC metabolites **12a**, **12b**, **12c**, **12a′**, and **12a″**.

acid to give **11a**, which was then reacted with iodomethane to give **12a**. Compound **14** was also coupled with **20** to give **2**. The disulfide of **24** was then reduced with DTT to give **11b**, which was reacted with iodomethane to give **12b**. The *S*-methylated metabolites could potentially be oxidized on their sulfur atoms in liver. Representative compounds **12a′** and **12a″** were prepared by oxidizing **12a** with *tert*-butyl hydroperoxide in the presence of vanadium acetylacetonate.

To determine if linker stereochemistry affected cytotoxicity, the anti-huEGFR immolative ADCs (**6a**–**6d**) were incubated with Ag+ CA922 cells, Figure 3A. Cytotoxicities for all ADCs were determined as previously described.[23] Conjugate **6d** (L, L, D) was the least potent, while the other conjugates exhibited similar high cytotoxicities. This indicated that ADC cytotoxicity was impaired when a D-alanine was directly attached to the immolative nitrogen, which will be designated as a D-linked conjugate. Conjugate **1a** also had similar potency as **6a**–**6c** against CA922 cells. In each case, the addition of a 1000-fold molar excess of the unconjugated anti-huEGFR antibody fully

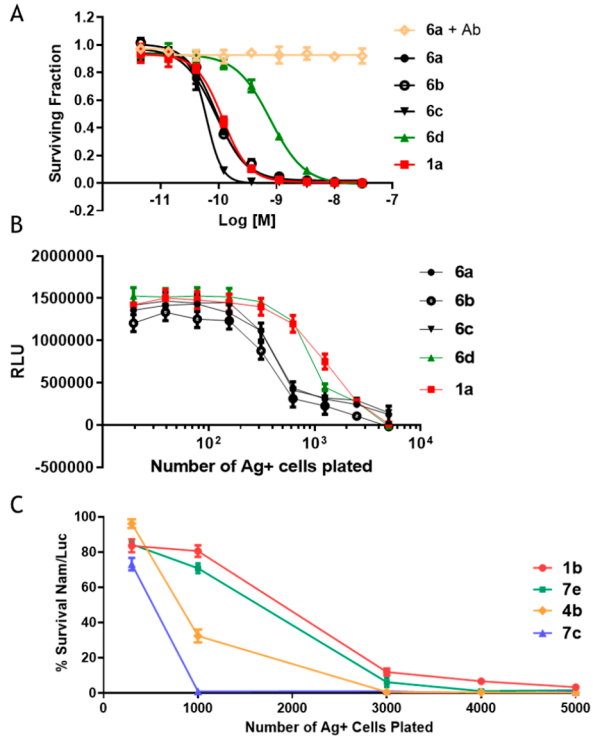

Figure 3. (A) *In vitro* cytotoxicities of immolative ADCs bearing peptides with different stereochemistries and of **1a** against CA922 cells. (**6a** + **Ab**) indicates **6a** plus 1000 equiv of anti-EGFR antibody. (B) Bystander killing (via assay 1) of immolative conjugates bearing peptides of different stereochemistries compared to **1a**. RLU indicates relative luminescence units. (C) *In vitro* bystander killing activity (via assay 2) of immolative ADCs that have different **n** values and the disulfide-linked ADC **1b**. The cell lines Jeg-3 cells (Ag+) and Nam \Luc (Ag−), which are Namalwa cells stably transfected with luciferase, were used.

inhibited ADC potency, demonstrating that cytotoxicity was antigen-dependent.

Next, the effect of methylene side chain length (**n**) on ADC cytotoxicity to cells that homogeneously express target antigen was investigated. The cytotoxicities of **7e** and **7c**, having **n** values of 3 and 5, respectively, were most often similar to each other, and to **1b** (Supplementary Table S1). ADCs **6a**–**6d** were tested for their ability to induce bystander killing *in vitro*, Figure 3B. A fixed number of Ag− cells were incubated with ADC and a variable number of Ag+ cells.[3] The Ag+ cells take up and degrade the ADC to release metabolite(s) that can kill these cells. Membrane permeable metabolite(s) may also diffuse into and kill a portion of the proximal Ag− cells (bystander cells). ADCs that induce the highest level of bystander killing require addition of the lowest number of added Ag+ cells to kill the Ag− cells in the mixed cell population. The relative number of HCC827 Ag+ cells needed to kill 50% of the MCF-7 Ag− cells were compared. Conjugates **6d** and **1a** required addition of ∼1250 Ag+ cells, while the other ADCs required only ∼400 Ag+ cells. Thus, **6a**, **6b**, and **6c** induced ∼3-fold greater *in vitro* bystander killing than **6d** and **1a**.

As shown in Figure 3C, increasing the number of methylene units in the maytansinoid side chain increased the *in vitro* bystander killing of immolative ADCs. Conjugates **7e** and **7c**, having 3 and 5 methylene groups in the maytansinoid side chain, required approximately 1800 and 700 Jeg-3 Ag+ cells,

DOI: 10.1021/acsmedchemlett.9b00310
ACS Med. Chem. Lett. 2019, 10, 1393−1399

respectively, to induce 50% Nam/Luc Ag− cell killing. Thus, **7c** induced ∼2.5-fold more bystander killing than **7e**. Conjugate **7c** also induced more bystander killing than **4b** and **1b**, which required approximately 950 and 2000 Ag+ cells, respectively, to induce 50% cell killing. The similar cytotoxicities of **7c** and **7e** could be explained if their metabolites are produced with similar efficiencies and have similar potencies once inside cells. However, if the metabolites of **7c** are more hydrophobic, as expected, then they could more easily diffuse into other cells to induce more bystander killing. Additional studies will be needed to determine if this is the case; however, because of their lower bystander killing, conjugates with **n** = 3 were not evaluated further.

The metabolites of **8c** were identified by incubating the conjugate with the high processing cell line COLO-205 for 24 h followed by cell lysis with organic solvent, using a previously described method.[8] As a control, COLO-205 cells were treated the same way but without prior exposure to **8c**. Both samples were analyzed by UPLC/MS (Supplementary Figure S1). The 252 nm UPLC trace of cells treated with **8c** showed two peaks that were not in the control, a major peak at 12.73 min and a minor peak at 7.72 min having about a fourth of the area of the major peak. The synthesized *S*-methylated standards **12a** and its sulfoxide **12a′**, shown in Figure 1D, were found to have the same retention times and mass spectra as the 12.73 and 7.72 min peaks, respectively. Sulfides are prone to air oxidation, and trace metals can act as catalysts.[24] Indeed aqueous solutions of standard **12a** were oxidized to **12a′** over time (data not shown). Indicating that **12a′** in cell lysates was likely an artifact due to oxidation of **12a** by air.

The *in vitro* cytotoxicities of the synthesized *S*-methylated metabolites **12a**−**12b** were evaluated on the H1703, H1975, and COLO-704 cell lines, Table 1. The potency of **12a** (**n** = 5) was consistently ∼2.5 times that of **12b** (**n** = 3), indicating that the cytotoxicity of free metabolites increased as hydrophobic methylene units were added. Also, **12a** had a similar potency to the isomeric compound **3b**. The synthesized sulfone **12a″** and the racemic sulfoxide **12a′** were at least 80-fold less cytotoxic than the precursor **12a**. Indicating that if **12a** is efficiently oxidized in liver it should be substantially inactivated.

Table 1. *In Vitro* Cytotoxicities of *S*-Methylated ADC Metabolites and the Oxidation Products of 12a (12a′ and 12a″)

	Cell Line IC_{50} (M)		
metabolite	H1703	H1975	COLO-704
12a (**n** = 5)	2.3×10^{-12}	2.5×10^{-12}	3.0×10^{-12}
12b (**n** = 3)	5.9×10^{-12}	5.6×10^{-12}	6.9×10^{-12}
3b	3.7×10^{-12}	4.1×10^{-12}	5.1×10^{-12}
12a′	3.1×10^{-10}	8.4×10^{-10}	8.2×10^{-10}
12a″	6.3×10^{-10}	2.1×10^{-10}	3.6×10^{-10}

Earlier studies with maytansinoid ADCs indicated mouse tolerabilities between 1200−1500 μg/kg based on the mass of delivered payload.[6,10] An initial study was conducted using anti-huEGFR ADCs (2 mice/group) at a dose of 1200 μg/kg based on the mass of delivered payload (47 mg/kg based on the mass of antibody) to determine if the tolerability of immolative conjugates was affected by having a single D-alanyl in the tripeptide linker and how these tolerabilities compared to a disulfide-linked ADC, Figure 4. The groups receiving vehicle, **1a**, and **6c** gained weight, although some skin reddening was noted in mice receiving **6c**. In contrast, animals that had been treated with **6a** and **6b** lost weight and displayed pronounced skin reddening. The mice in the **6d** group, D-linked conjugate, also displayed some skin toxicity, but weight loss was not as pronounced as the **6a** and **6b** groups. This study revealed that immolative ADCs bearing the L-Ala-D-Ala-L-Ala linker were better tolerated in mice than those bearing the other tripeptide linkers.

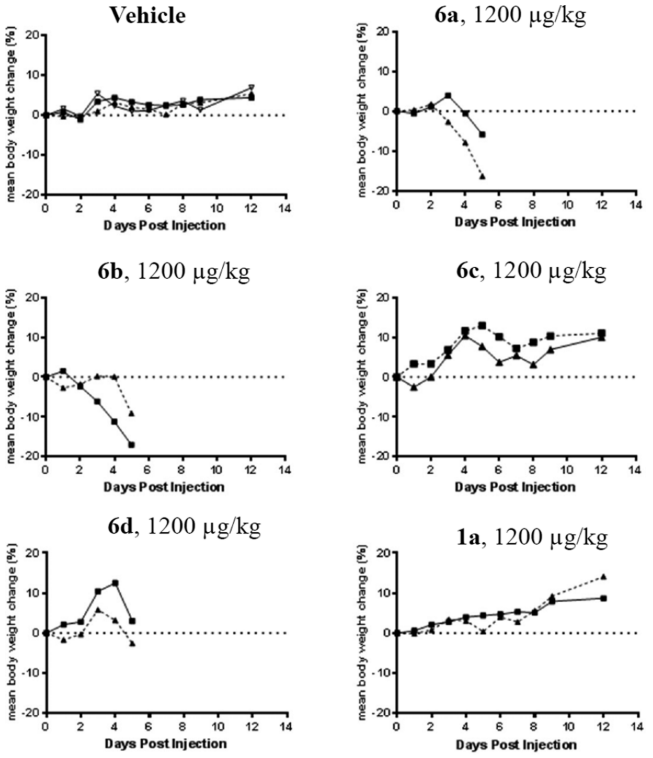

Figure 4. Change in body weight of CD-1 mice treated with vehicle (3 mice/group), the immolative ADCs **6a**−**6d** (2 mice/group), or with the disulfide-linked ADC **1a** (2 mice/group).

A second MTD study was undertaken, using ADCs bearing an anti-huFR*α* antibody, Figure 5A. The groups (8 mice/group) consisted of vehicle, **4b** (1250 μg/kg), and the immolative ADC **7c** (L, D, L) at 1000 and 1250 μg/kg. Mice in all groups gained weight, but the **7c** (1250 μg/kg) group had some skin reddening. Because of their favorable tolerability, immolative ADCs bearing the L-Ala-D-Ala-L-Ala peptide were evaluated in further *in vivo* studies.

The clearance of **7c** at a dose of 10 mg/kg from circulation in nontumor bearing mice was determined by ELISA as previously described.[25] The half-lives of the ADC's antibody and drug components were ∼15.2 and ∼10.9 days, respectively, Figure 5B.

The *in vivo* efficacy of maytansinoid ADCs **9c** and **1d** was compared in mice (8/group) bearing Hs 746T tumor xenografts, where the target c-Met antigen is expressed homogeneously, Figure 6A. The H-Score for these cells,[26] a measure of antigen expression, is 160. At the 2.5 mg/kg dose, complete regressions (CRs) were achieved for all mice in the **9c** group, but only two CRs were seen in the **1d** group, which latter regrew. Next anti-huCanAg ADCs (5 mg/kg) were compared in mice (6/group) bearing HT-29 xenografts, where CanAg is only expressed on 20−30% of cancer cells in the tumor, Figure 6B.[27] The greatest antitumor activity was observed with the immolative ADCs **8a** (L, L, L) and **8c** (L, D,

DOI: 10.1021/acsmedchemlett.9b00310
ACS Med. Chem. Lett. 2019, 10, 1393−1399

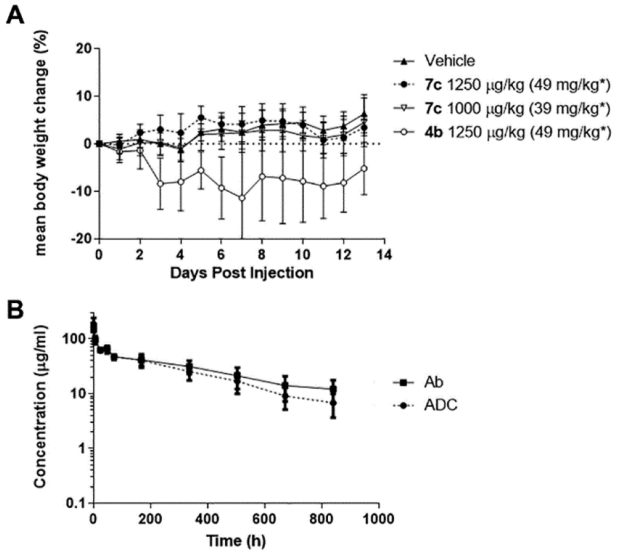

Figure 5. (A) *In vivo* tolerability in mice (8/group) of the immolative ADC **7c** vs the anilino ADC **4b** and vehicle. * indicates the concentration of ADC based on the antibody component. (B) Pharmacokinetic study of **7c** in mice where ■ is the concentration versus time plot of the antibody component and ● is the concentration versus time plot of the payload component.

L), resulting in CRs in 6/6 mice, although tumors began to regrow at day 30. The anilino ADC **4c** (2/6 CRs) and the disulfide-linked ADC **1c** (0/6 CRs) were less efficacious. HT-29 xenograft bearing mice (6/group) were also treated at 2.5 mg/kg; group **8c** (2 CRs) had a larger reduction in median tumor size than group **8a** (1 CR), Figure 6C. The *in vivo* efficacy of anti-huFRα ADC was compared in mice bearing OV-90 xenografts, which express folate receptor heterogeneously (H-Score = 48), Figure 6D. The immolative ADC **7c** was approximately twice as efficacious as the anilino ADC **4b**, based on the similarity in the tumor volume plots for group **7c** (1.25 mg/kg) and group **4b** (2.5 mg/kg), and the similar or better response of group **7c** (2.5 mg/kg) compared to group **4b** (5 mg/kg).

In conclusion, the *in vitro* bystander killing of immolative ADCs positively correlated with metabolite hydrophobicity. Conjugates with adjacent linker L-alanyl residues were not as well tolerated and were less efficacious than the (L-Ala-D-Ala-L-Ala) peptide-linked ADC. We postulate that ADCs with adjacent L-alanyl residues may be less stable *in vivo*, which would increase metabolite release in healthy tissues, and lower payload delivery to tumors. Finally, increasing both *in vitro* bystander killing, and linker stability resulted in ADCs having a better therapeutic window in mice than previously described maytansinoid conjugates.

■ ASSOCIATED CONTENT

Supporting Information

The Supporting Information is available free of charge on the ACS Publications website at DOI: 10.1021/acsmedchemlett.9b00310.

Detailed experimental procedures(PDF)

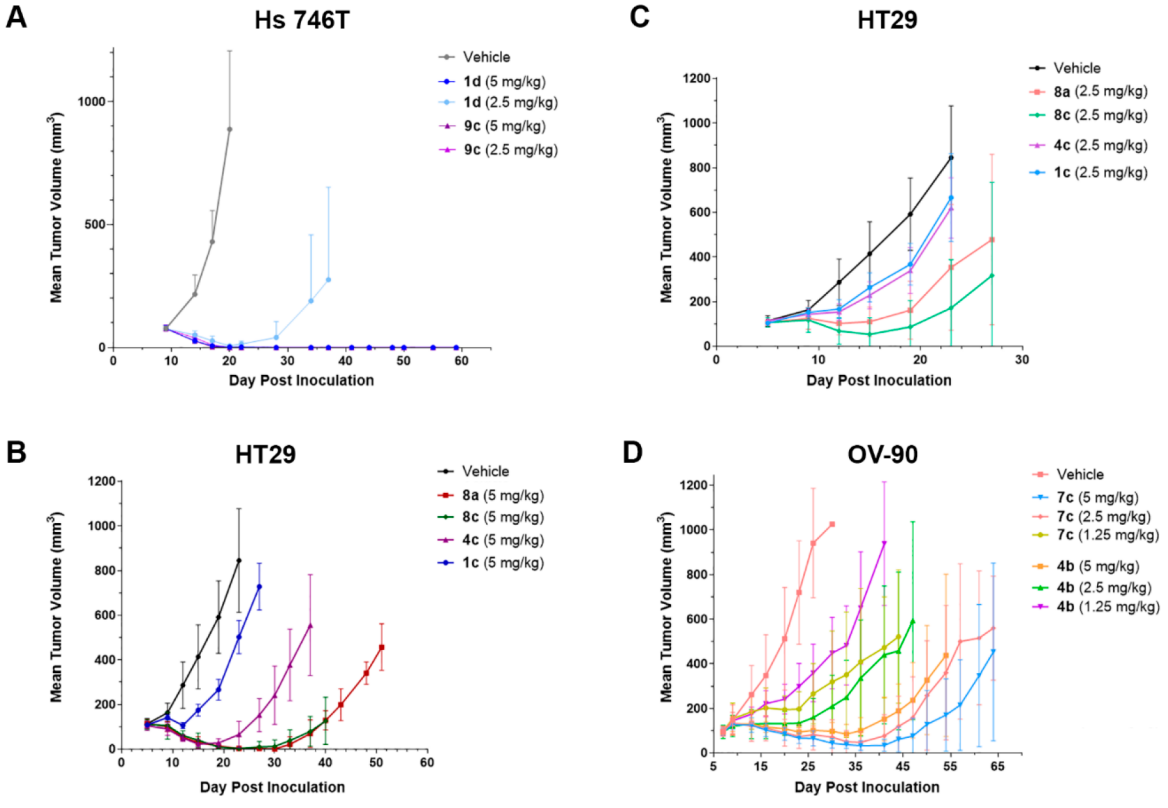

Figure 6. *In vivo* efficacy of maytansinoid ADCs against (A) homogeneously expressing mouse Hs746T xenografts (8 mice/group), (B) heterogeneously expressing HT-29 xenografts (6 mice/group, 5 mg/kg), (C) heterogeneously expressing HT-29 xenografts (6 mice/group, 2.5 mg/kg), and (D) heterogeneously expressing OV-90 xenografts (6 mice/group).

DOI: 10.1021/acsmedchemlett.9b00310
ACS Med. Chem. Lett. 2019, 10, 1393−1399

AUTHOR INFORMATION

Corresponding Author

*E-mail: waynecwiddison@gmail.com.

ORCID

Wayne C. Widdison: 0000-0003-2463-1440

Author Contributions

The manuscript was written through contributions of all authors. All authors have given approval to the final version of the manuscript.

Funding

This study was supported by ImmunoGen, Inc.

Notes

The authors declare no competing financial interest.

ACKNOWLEDGMENTS

We would like to thank Richard Bates for editing of the manuscript, Shan Jin for analysis of metabolites, Erica Hong for the preparation of some ADCs used in this work, and Richard Gregory, Joseph Kenny, and David Pleynet for helpful suggestions.

ABBREVIATIONS

ADC, antibody−drug conjugate; CR, complete regression (tumor xenograft no longer detected); DIPEA, *N*,*N*-diisopropylethylamine; DMF, dimethylformamide; DTT, 1,4-dithiothreitol; EDC, 1-ethyl-3-(3-(dimethylamino)propyl)-carbodiimide; PR, partial regression (50% reduction of tumor xenograft size); Et_3N, triethylamine; SEC, size-exclusion chromatography; TFA, trifluoroacetic acid

REFERENCES

(1) Dan, N.; Setua, S.; Kashyap, V. K.; Khan, S.; Jaggi, M.; Yallapu, M. M.; Chauhan, S. C. Antibody-drug conjugates for cancer therapy: chemistry to clinical implications. *Pharmaceuticals (Basel)* **2018**, *11*, E32.

(2) Bargh, J. D.; Isidro-Llobet, A.; Parker, J. S.; Spring, D. R. Cleavable linkers in antibody−drug conjugates. *Chem. Soc. Rev.* **2019**, *48*, 4361.

(3) Kovtun, Y. V.; Audette, C. A.; Ye, Y.; Xie, H.; Ruberti, M. F.; Phinney, S. J.; Leece, B. A.; Chittenden, T.; Blaettler, W. A.; Goldmacher, V. S. Antibody-drug conjugates designed to eradicate tumors with homogeneous and heterogeneous expression of the target antigen. *Cancer Res.* **2006**, *66*, 3214.

(4) Girish, S.; Gupta, M.; Wang, B.; Lu, D.; Krop, I. E.; Vogel, C. L.; Burris, H. A., Iii; LoRusso, P. M.; Yi, J. H.; Saad, O.; Tong, B.; Chu, Y. W.; Holden, S.; Joshi, A. Clinical pharmacology of trastuzumab emtansine (T-DM1): an antibody-drug conjugate in development for the treatment of HER2-positive cancer. *Cancer Chemother. Pharmacol* **2012**, *69*, 1229.

(5) de Goeij, B. E.; Lambert, J. M. New developments for antibody-drug conjugate-based therapeutic approaches. *Curr. Opin. Immunol.* **2016**, *40*, 14.

(6) Kellogg, B. A.; Garrett, L.; Kovtun, Y.; Lai, K. C.; Leece, B.; Miller, M.; Payne, G.; Steeves, R.; Whiteman, K. R.; Widdison, W.; Xie, H.; Singh, R.; Chari, R. V.; Lambert, J. M.; Lutz, R. J. Disulfide-linked antibody-maytansinoid conjugates: optimization of in vivo activity by varying the steric hindrance at carbon atoms adjacent to the disulfide linkage. *Bioconjugate Chem.* **2011**, *22*, 717.

(7) Drake, P. M.; Rabuka, D. An emerging playbook for antibody−drug conjugates: lessons from the laboratory and clinic suggest a strategy for improving efficacy and safety. *Curr. Opin. Chem. Biol.* **2015**, *28*, 174.

(8) Erickson, H. K.; Park, P. U.; Widdison, W. C.; Kovtun, Y. V.; Garrett, L. M.; Hoffman, K.; Lutz, R. J.; Goldmacher, V. S.; Blattler, W. A. Antibody-maytansinoid conjugates are activated in targeted cancer cells by lysosomal degradation and linker-dependent intracellular processing. *Cancer Res.* **2006**, *66*, 4426.

(9) Sun, X.; Widdison, W.; Mayo, M.; Wilhelm, S.; Leece, B.; Chari, R.; Singh, R.; Erickson, H. Design of antibody-maytansinoid conjugates allows for efficient detoxification via liver metabolism. *Bioconjugate Chem.* **2011**, *22*, 728.

(10) Widdison, W. C.; Ponte, J. F.; Coccia, J. A.; Lanieri, L.; Setiady, Y.; Dong, L.; Skaletskaya, A.; Hong, E. E.; Wu, R.; Qiu, Q.; Singh, R.; Salomon, P.; Fishkin, N.; Harris, L.; Maloney, E. K.; Kovtun, Y.; Veale, K.; Wilhelm, S. D.; Audette, C. A.; Costoplus, J. A.; Chari, R. V. Development of anilino-maytansinoid ADCs that efficiently release cytotoxic metabolites in cancer cells and induce high levels of bystander killing. *Bioconjugate Chem.* **2015**, *26*, 2261.

(11) Ponte, J. F.; Sun, X.; Yoder, N. C.; Fishkin, N.; Laleau, R.; Coccia, J.; Lanieri, L.; Bogalhas, M.; Wang, L.; Wilhelm, S.; Widdison, W.; Pinkas, J.; Keating, T. A.; Chari, R.; Erickson, H. K.; Lambert, J. M. Understanding how the stability of the thiol-maleimide linkage impacts the pharmacokinetics of lysine-linked antibody-maytansinoid conjugates. *Bioconjugate Chem.* **2016**, *27*, 1588.

(12) Kingsbury, W. D.; Boehm, J. C.; Perry, D.; Gilvarg, C. Portage of various compounds into bacteria by attachment to glycine residues in peptides. *Proc. Natl. Acad. Sci. U S A* **1984**, *81*, 4573.

(13) Lai, K. C.; Deckert, J.; Setiady, Y. Y.; Shah, P.; Wang, L.; Chari, R.; Lambert, J. M. Evaluation of targets for maytansinoid ADC therapy using a novel radiochemical assay. *Pharm. Res.* **2015**, *32*, 3593.

(14) Ab, O.; Whiteman, K. R.; Bartle, L. M.; Sun, X.; Singh, R.; Tavares, D.; LaBelle, A.; Payne, G.; Lutz, R. J.; Pinkas, J.; Goldmacher, V. S.; Chittenden, T.; Lambert, J. M. IMGN853, a Folate receptor-alpha (FRalpha)-targeting antibody-drug conjugate, exhibits potent targeted antitumor activity against FRalpha-expressing tumors. *Mol. Cancer Ther.* **2015**, *14*, 1605.

(15) Tolcher, A. W.; Ochoa, L.; Hammond, L. A.; Patnaik, A.; Edwards, T.; Takimoto, C.; Smith, L.; de Bono, J.; Schwartz, G.; Mays, T.; Jonak, Z. L.; Johnson, R.; DeWitte, M.; Martino, H.; Audette, C.; Maes, K.; Chari, R. V.; Lambert, J. M.; Rowinsky, E. K. Cantuzumab mertansine, a maytansinoid immunoconjugate directed to the CanAg antigen: a phase I, pharmacokinetic, and biologic correlative study. *J. Clin. Oncol.* **2003**, *21*, 211.

(16) Lai, K. C.; Li, M.; Selvitelli, K.; Sikka, S.; Boulé, S.; Gavrilescu, L. C.; Hicks, S. W.; Donahue, K. Abstract 4817: Preclinical evaluation of a new, non-agonist ADC targeting MET amplified tumors with a peptide-linked maytansinoid. *Cancer Res.* **2019**, *79*, 1.

(17) Doronina, S. O.; Bovee, T. D.; Meyer, D. W.; Miyamoto, J. B.; Anderson, M. E.; Morris-Tilden, C. A.; Senter, P. D. Novel peptide linkers for highly potent antibody-auristatin conjugate. *Bioconjugate Chem.* **2008**, *19*, 1960.

(18) Bennion, B. J.; Be, N. A.; McNerney, M. W.; Lao, V.; Carlson, E. M.; Valdez, C. A.; Malfatti, M. A.; Enright, H. A.; Nguyen, T. H.; Lightstone, F. C.; Carpenter, T. S. Predicting a drug's membrane permeability: A computational model validated with in vitro permeability assay data. *J. Phys. Chem. B* **2017**, *121*, 5228.

(19) Akssira, M.; Boumzebra, M.; Kasmi, H.; Dahdouh, A. New Routes to 1,4- Benzodiazepin-2,5-diones. *Tetrahedron* **1994**, *50*, 9051.

(20) Benoiton, L. *Chemistry of Peptide Synthesis*; CRC Press, 2006.

(21) Kumar, N. S.; Ratnayake, R. M.; Widmalm, G.; Jansson, P. E. Selective cleavage of welan gum (S-130) by oxidative decarboxylation with lead tetraacetate. *Carbohydr. Res.* **1996**, *291*, 109.

(22) Widdison, W. C.; Wilhelm, S. D.; Cavanagh, E. E.; Whiteman, K. R.; Leece, B. A.; Kovtun, Y.; Goldmacher, V. S.; Xie, H.; Steeves, R. M.; Lutz, R. J.; Zhao, R.; Wang, L.; Blattler, W. A.; Chari, R. V. Semisynthetic maytansine analogues for the targeted treatment of cancer. *J. Med. Chem.* **2006**, *49*, 4392.

(23) Kovtun, Y. V.; Audette, C. A.; Mayo, M. F.; Jones, G. E.; Doherty, H.; Maloney, E. K.; Erickson, H. K.; Sun, X.; Wilhelm, S.; Ab, O.; Lai, K. C.; Widdison, W. C.; Kellogg, B.; Johnson, H.; Pinkas, J.; Lutz, R. J.; Singh, R.; Goldmacher, V. S.; Chari, R. V. Antibody-maytansinoid conjugates designed to bypass multidrug resistance. *Cancer Res.* **2010**, *70*, 2528.

DOI: 10.1021/acsmedchemlett.9b00310
ACS Med. Chem. Lett. 2019, 10, 1393−1399

(24) Hoffmann, M. R.; Lim, B. C. Kinetics and mechanism of the oxidation of sulfide by oxygen: catalysis by homogeneous metal-phthalocyanine complexes. *Environ. Sci. Technol.* **1979**, *13*, 1406.
(25) Xie, H.; Audette, C.; Hoffee, M.; Lambert, J. M.; Blattler, W. A. Pharmacokinetics and biodistribution of the antitumor immunoconjugate, cantuzumab mertansine (huC242-DM1), and its two components in mice. *J. Pharmacol. Exp. Ther.* **2004**, *308*, 1073.
(26) Detre, S.; Saclani Jotti, G.; Dowsett, M. A ″quickscore″ method for immunohistochemical semiquantitation: validation for oestrogen receptor in breast carcinomas. *J. Clin. Pathol.* **1995**, *48*, 876.
(27) Liu, C.; Tadayoni, B. M.; Bourret, L. A.; Mattocks, K. M.; Derr, S. M.; Widdison, W. C.; Kedersha, N. L.; Ariniello, P. D.; Goldmacher, V. S.; Lambert, J. M.; Blattler, W. A.; Chari, R. V. Eradication of large colon tumor xenografts by targeted delivery of maytansinoids. *Proc. Natl. Acad. Sci. U. S. A.* **1996**, *93*, 8618.

DOI: 10.1021/acsmedchemlett.9b00310
ACS Med. Chem. Lett. 2019, 10, 1393−1399